Azatriseptanes - strained framework analogs of [7,7,7]circulenes

Kai Zhang,[a]‡ Philip A. Hope,[a] ‡ Mélissa El Bitar Nehme,[a] Anthony Linden,[a] Bernhard Spingler,[a] and Michel Rickhaus*[a]

‡ These authors contributed equally

[a] K. Zhang, Dr. P. A. Hope, M. El Bitar Nehme, Prof. Dr. Anthony Linden, Prof. Dr. Bernhard Spingler, Dr. M. Rickhaus
Department of Chemistry | University of Zurich | Winterthurerstrasse 190, 8057 Zurich, Switzerland
E-mail: michel.rickhaus@chem.uzh.ch

Abstract: *The syntheses and characterizations of heptagon-embedded polycyclic aromatic compounds are essential for understanding the effect of negative curvature on carbon allotropes such as fullerene and graphene that have applications in functional organic materials. However, owing to the synthetic difficulties in functionalizing and embedding 7-membered rings, these strain-challenged structures are relatively unexplored. We report here the synthesis and photophysical characterization of a triarylamine core bridged with ethane chains at the 2,2'-positions. In doing so, we provide access to the first heterocycle containing three fused heptagon rings with a nitrogen at its core (**BATA-NHAc**). DFT calculations and X-ray crystallography reveal a remarkably strained structure wherein two of the bridged aryl units approach coplanarity, whilst the third ring is twisted out of plane. The unique conformation of **BATA-NHAc** results in distinctive photophysical and electrochemical properties that open new avenues in understanding the structure-property relationships of curved π-aromatics and the construction of π-frameworks of increasing complexion.*

Though synthetically challenging, curved polycyclic aromatics offer not only aesthetic appeal, but are also ideal model systems to relate structure and curvature to optical and electronic properties.[1] One way to induce curvature in flat polycyclic aromatic hydrocarbons (PAHs) is by embedding non-hexagonal rings into graphene-type nanocarbons.[2] The introduction of a pentagon typically results in positive curvature in the form of a bowl.[3] Ring sizes larger than six (heptagons, octagons, etc.) lead to negative curvature and often saddle-like structures.[1c, 4] While bowl-shaped nanographenes have been successfully used as templates for nanotubes,[5] negative curvatures are particularly appealing because they lead to contorted but formally infinite surfaces. Theoretical three-dimensional (3D) carbon allotropes like Mackay crystals,[6] Schwarzites,[7] toroids, and peanut-shaped tubulenes[8] feature one or several fused seven-membered rings in their repeating unit cell. It speaks of the synthetic challenge of these motifs that while polyquinines (the hydrogenated framework of annelated pentagons) have been known for decades, there exist only three examples that feature more than two annelated seven-membered hydrocarbon rings.[9]

Among the hallmark examples of saddle-shaped seven-membered PAHs are [7]circulene[10] (Figure 1a, left) and [7,7]circulene[11] (Figure 1a, middle) which are composed of one and two heptagon rings respectively, with the latter sharing one

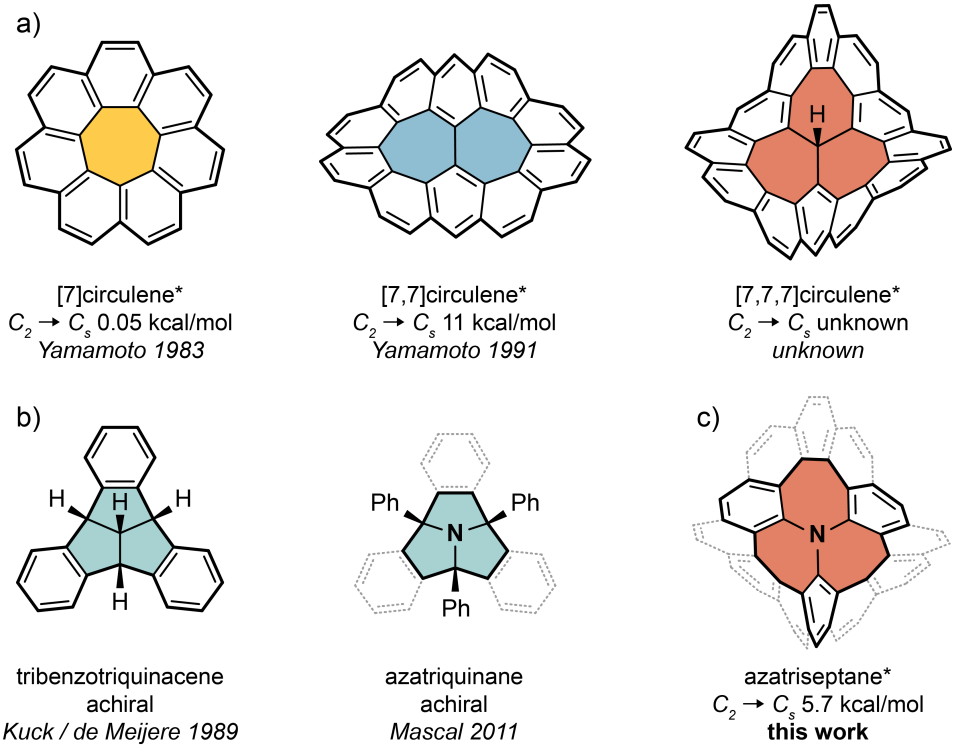

Figure 1. a) Structures of previously reported heptagon-embedded PAHs (left and middle) versus a newly proposed theoretical PAH (right); b) structures of tribenzotriquinacene (left) and azatriquinane (right); c) molecular structure of azatriseptane. * indicates chirality of the lowest energy conformer.

C-C bond of the heptagons. Both circulenes are chiral in their ground state, however [7]circulene is classified as stereochemically fluctuating as a result of its low racemization barrier (0.05 kcal/mol).[12] Notably, the racemization pathway from C_2 via the C_s symmetric intermediate is similar for the π-extended [7,7]circulene, although different in energy.[13] Extension of annelation appears synthetically challenging and the racemization energies and pathways of these polyseptanes remain largely unexplored.

A possible approach to higher septanes may arise by considering tribenzotriquinacene[14] – a compound containing three fused pentagon rings sharing one sp^3 carbon. This compound becomes chiral only through substitution[15] with the framework reminiscent of bowl-shaped nanographenes.

Here we report the first syntheses of higher septanes featuring three seven-membered rings surrounding a central nitrogen. Each ring shares a carbon-nitrogen bond with the other two, which results in a (hypothetical) triseptane with a central sp^2-nitrogen. Formal substitution of this central insulator with a nitrogen results in the current azatriseptane, in analogy to azatriquinane.[15b]

We present the synthesis of a family of *N*-centered heptagon fused triarylamines (labeled **BATA** for ***b***ridged ***a***rylamine ***t***ris***a***mide, scheme 1), their structural analysis, optical and electrochemical properties. Single crystal X-ray diffraction (SC-XRD) analysis and density functional theory (DFT) calculations show they adopt saddle-shaped, strained conformers that significantly differ from the typical propeller structure of triarylamines. **BATA-NHAc**, the derivative with acetamides in the para-positions of the aryl rings, shows bathochromic shifts and concentration-dependent emission profiles. These features underline the possible application of our compounds as functional organic molecules in supramolecular materials.

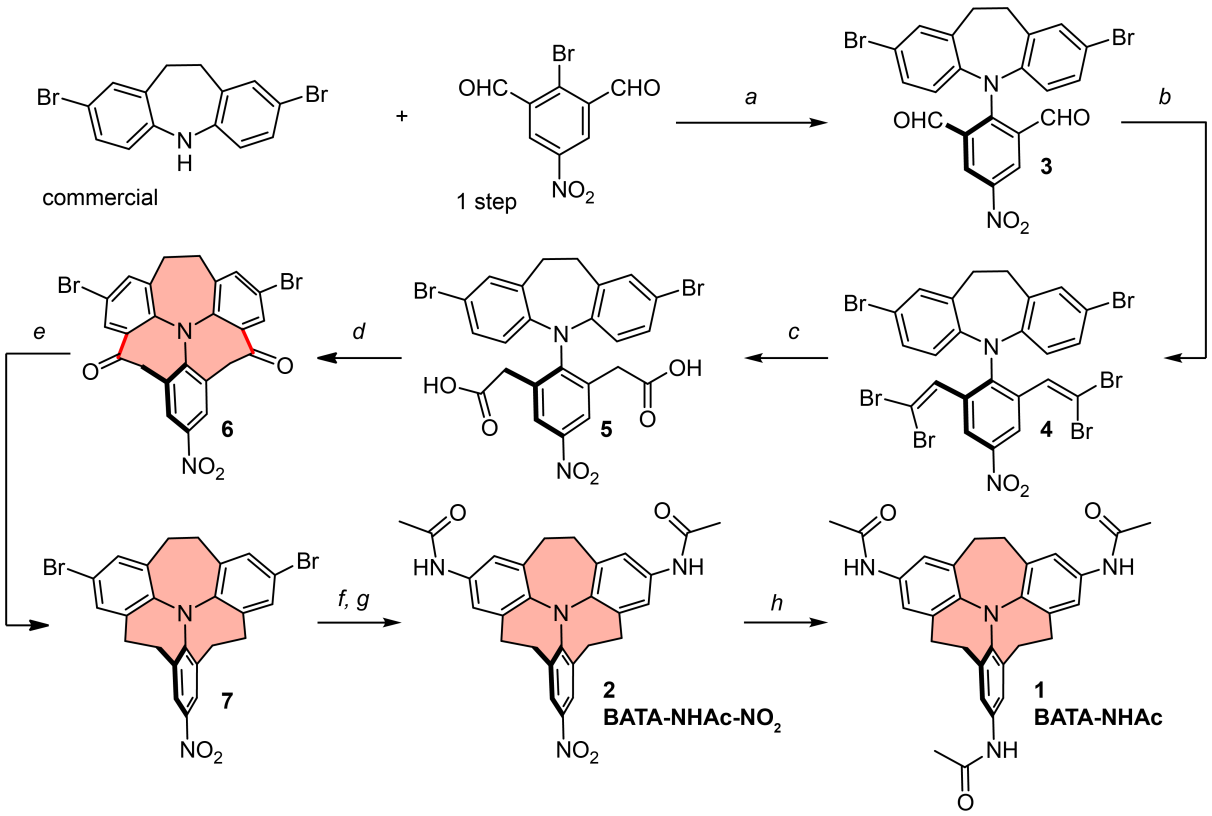

Scheme 1. Synthesis of **BATA-NHAc**. Reagents and conditions: a) CsF, DMF, 125 °C, 12 hrs; b) CBr_4/PPh_3, DCM, 0 °C-r.t, 3 hrs; c) KOH/MeOH, THF/H_2O, 70 °C, 48 hrs; d) 1. DCM/$(COCl)_2$, 2. $AlCl_3$, DCE, 0 °C-r.t, 24 hrs; e) $AlCl_3$/$HSiEt_3$, DCM, 0 °C-r.t, 4 hrs; f) 1. Benzophenone imine, BINAP, $Pd_2(dba)_3$, NaO^tBu, toluene, 0 °C, 12 hrs, 2. HCl (2N), THF, r.t, 4 hrs; g) Acetyl chloride, DCM/TEA, 0 °C-r.t, 12 hrs; h) 1. Pd/C, H_2, EtOAc/MeOH, r.t, 12 hrs, 2. Acetyl chloride, DCM/TEA, r.t, 12 hrs.

The synthetic route towards **BATA-NHAc** is shown in Scheme 1. Starting from the two literature-known compounds dibromo azepine and dialdehyde and taking advantage of the electron-deficient nature of the latter, compound **3** is efficiently obtained in 67% yield by nucleophilic aromatic substitution. Inspired by *Kim et al.*'s[16] one-carbon elongation of aryl aldehydes, we developed an efficient and rapid homologation of dialdehyde **3** to the corresponding diacid **5** via a two-step reaction sequence. First, dialdehyde **3** is reacted with CBr_4/PPh_3 to yield compound **4**. Then, treatment of compound **4** with KOH/MeOH in aq. THF yields cyclization precursor **5** which is directly carried on without further

purification. Cyclization to the strained seven-membered framework is surprisingly efficient (65%) under classic Friedel-Crafts acylation conditions. The correct cyclization mode of diketone compound **6** was confirmed by SC-XRD (see Figure S21). The subsequent reduction of the two carbonyls in the presence of both bromine and nitro groups proved to be one of the most challenging steps in our synthetic route. After a thorough screening of conditions (see Table S1), we were glad to see that the use of $AlCl_3$ as a Lewis acid and $SiEt_3H$ as a hydride donor affords **7** in good (43%) yield considering the poor steric accessibility. The structure of the desired azatriseptane framework was confirmed by single crystal analysis of **7** (see Figure S23) and we were delighted to see that this compound was bench-stable under light and ambient conditions for weeks. Exposure of **7** to benzophenone imine in the presence of BINAP and NaO^{t}Bu allows the two-fold Buchwald-Hartwig amination to proceed smoothly to give the nitro-diamine intermediate. Following acetyl protection of the diamines, **BATA-NHAc-NO$_2$** was subjected to palladium-catalyzed hydrogenation which afforded the asymmetric monoamine intermediate which was readily acetyl-protected to furnish the target compound **BATA-NHAc**.

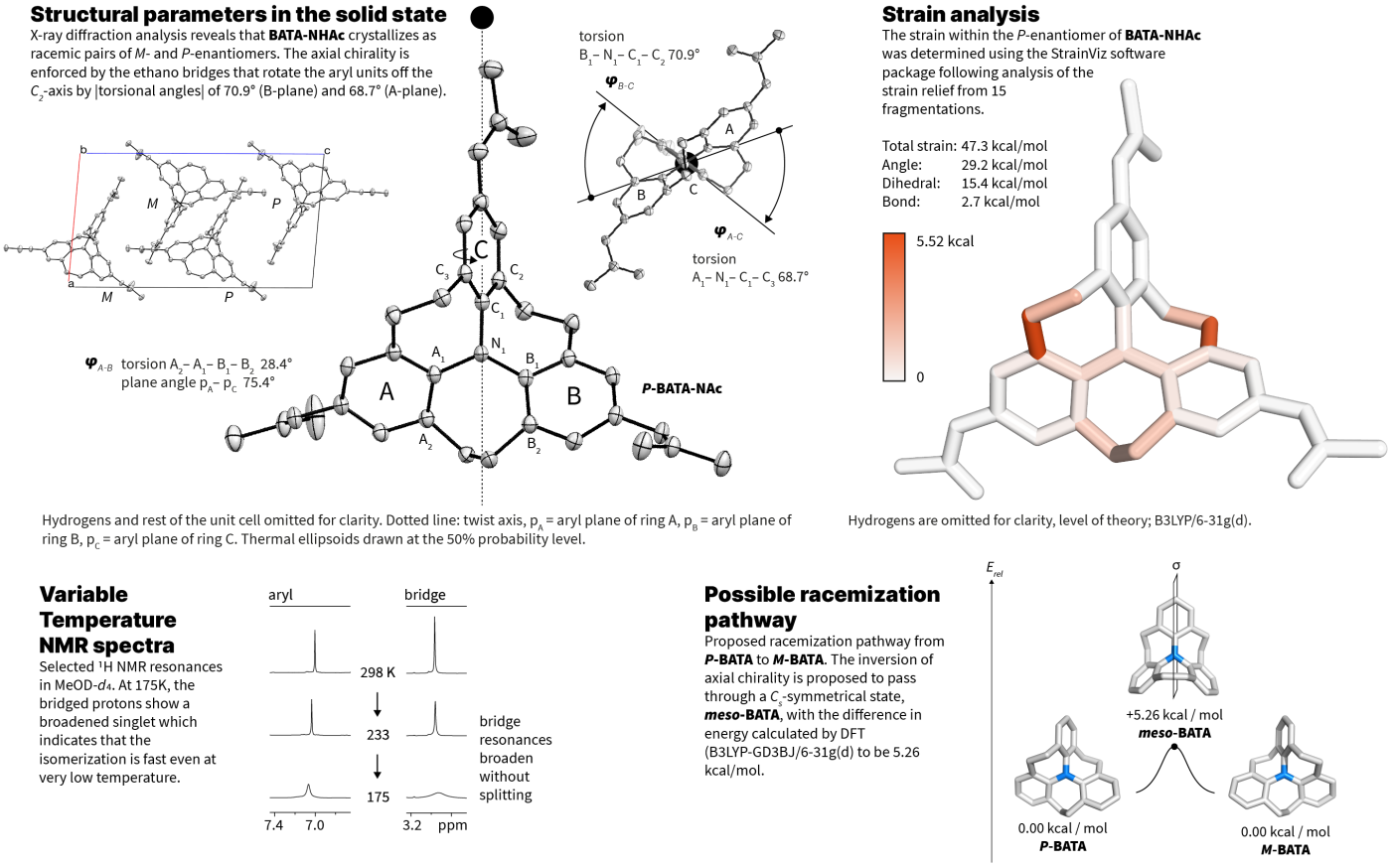

Figure 2. Crystal structure of *M*-**BATA-NHAc** and strain bond map and total strain energy. Variable temperature ^{1}H NMR spectra of **BATA-NHAc** (500 MHz, CD_3OD). The inversion pathway between the *M*- and *P*-triseptane framework as calculated by DFT (B3LYP-GD3BJ/6-31G(d)).

A single crystal of **BATA-NHAc** was obtained by slow evaporation of a toluene–methanol solution containing **BATA-NHAc**. The crystal structure exhibits (Figure 2) a saddle-shaped, near-perfect C_2-symmetric conformation as opposed to a C_3-symmetrical propeller that is typically observed for unbridged triphenylamines (**TPA**).[17] We find (Figure 2) helical chirality in **BATA-NHAc** with torsion around the C_2 axis. Torsional angles are 68.7° (A-plane) and 70.9° (B-plane) for the aryl units off the C_2-axis (C-plane). Both *P*-**BATA-NHAc** and *M*-**BATA-NHAc** (Figure 2) enantiomers are observed in the unit cell, packing as racemic pairs. Two of the bridged aryl units (A- and B-plane) within **BATA-NHAc** are close to planar with respect to the three sp^2 hybridized carbons directly attached to the nitrogen, at angles of rotation 26° (B-plane) and 35° (A-plane). The remaining aryl unit on the C_2-axis is twisted at 70° (C-plane). These angles deviate considerably from those observed in **TATA-NHAc**.[18] (plane–plane: 30–41°) which shows that the ethano bridges within **BATA-NHAc** have a detrimental impact on the conformation of the three aryl units. On closer inspection, distortion in the planarity of the aryl units in the A- and B-plane was observed, hinting at persistent strain in the A-B framework. We expanded the StrainViz software developed by Jasti and coworkers[19] to include multiply constrained systems and found it suitable to map strain within **BATA-NHAc** (see SI for supporting discussion). The total strain energy for **BATA-NHAc** was calculated (B3LYP/6-31g(d)) as 47.3 kcal/mol which is comparative to strained macrocycles such as Bodwell's naphthalene paracyclophane.[19] The strain map (Figure 2) shows that the strain is mostly localized in the ethano bridges that connect the aryl units in the A- and B-planes to the perpendicular aryl unit in the C-plane, with minor contributions in the third ring and the A/B aryls. Ring C is unaffected by strain. No significant intermolecular forces were observed in the packing (see Figure S26) of the crystal structure that may influence the conformation and therefore the strain in the molecule.

DFT (B3LYP-GD3BJ/6-31g(d)) was utilized to investigate the interconversion between the *P*- and *M*-isomers of the triseptane framework. It seemed logical to assume a $C_2 \rightarrow C_S$ transition, in line with [7]- and [7,7]circulene. The lowest energy conformation of **BATA** (Figure 2, not synthesized) was calculated and compared to the energy of the suspected transition state[9b] to derive a barrier to racemization of 5.3 kcal/mol. This low energy barrier can be correlated to the VT-NMR, which shows signal broadening upon lowering the temperature to 175 K, without reaching coalescence. These data suggest that inversion of helicity still occurs at low temperatures, significantly lower than for other molecules that display dynamic axial chirality such as bridged biphenyls.[20] The synthetic intermediate **BATA-NHAc-NO_2** also shows a similarly collapsed ^{1}H NMR singlet resonance at ambient temperature. Upon cooling, the spectrum becomes broad and more complex – due to the asymmetric nature of **BATA-NHAc-NO_2** it is challenging to assign this to a shifted barrier with certainty. We are currently investigating this in more detail.

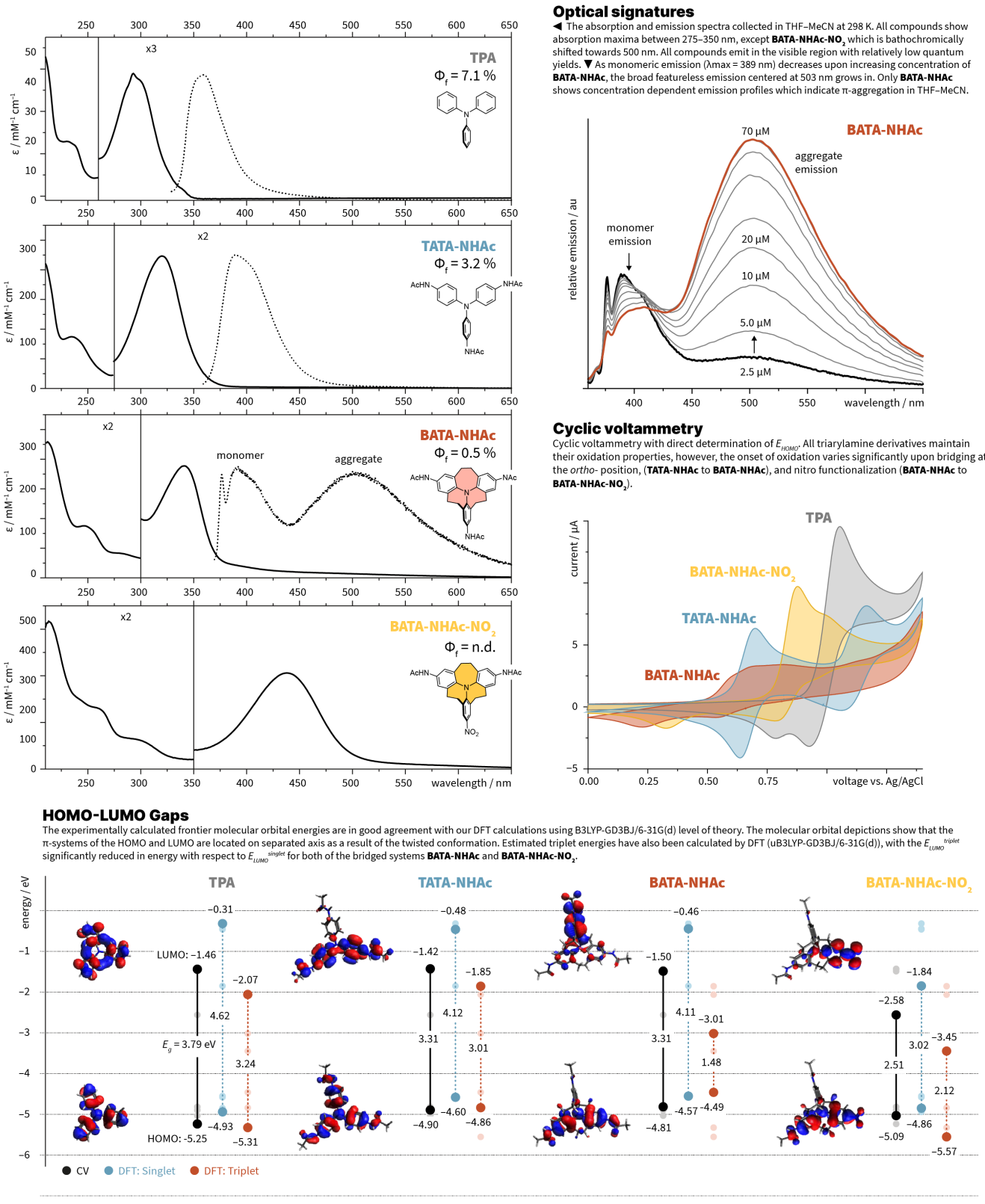

Figure 3. UV-vis (bold) and fluorescence spectra (dashed) collected in THF–MeCN (1:1 *v*/*v*); *c* = 2.5 µM (top left), *c* = variable conc. for **BATA-NHAc** (top right). Cyclic voltammograms collected in THF–MeCN (1:1 *v*/*v*) containing 0.1 M tetrabutyl ammonium hexfluorophosphate ($TBAPF_6$) as the supporting electrolyte; *c* = 0.3 mM and scan rate 100 mV s^{-1} (middle right); Frontier molecular orbital energy diagram and orbital depictions as calculated by DFT (dashed line) and experimentally by CV and onset of absorption (bold line).

The photophysical properties of **BATA-NHAc** were investigated in a mixture of THF–MeCN (1:1 *v/v*) and compared with baseline compounds **TPA** and **TATA-NHAc** as well as the push-pull system **BATA-NHAc-NO_2**. As shown in Figure 3, **BATA-NHAc** shows a broad absorption band centered at 339 nm, which is bathochromically shifted in comparison to non-bridged **TATA-NHAc** ($\Delta\lambda_{max}$ = 18 nm). Moreover, a weaker broad absorption band at 375–450 nm is observed for **BATA-NHAc** that is not present in **TATA-NHAc** at similar concentration. It was further found that **BATA-NHAc** exhibits concentration-dependent emission profiles, with a broad featureless emission at $\lambda_{em,\,max}$ = 503 nm growing in at higher concentrations (up to 70 µM) in favor of the monomer emission at $\lambda_{em,\,max}$ = 370 nm. The quantum yield of **BATA-NHAc** was determined to be 0.5%, i.e., almost non-emissive and significantly less than **TATA-NHAc** at 3.2%. These data suggest the conformation induced by the ethano bridges may play an important role in the self-assembly properties of **BATA-NHAc**. The tailoring of the optical properties of these systems by peripheral substitution was exemplified by **BATA-NHAc-NO_2** which absorbs in the visible region (350–520 nm) and exhibits complete quenching of emission that may be correlated to inter-system crossing (ISC) or internal conversion (IC), as observed for other nitro-containing compounds.[21]

Cyclic voltammetry was carried out in a mixture of THF–MeCN (1:1 *v/v*) and the onset of oxidation ($E_{onset,\,ox}$), and therefore E_{HOMO}, calculated. The effect of para-amide substitution is evident (Figure 3) with an increase in the E_{HOMO} to –4.90 eV for **TATA-NHAc** from –5.25 eV (**TPA**); the dicationic state is pseudo-reversible for the former, as observed for other substituted TATA derivatives.[22] The bridged system in **BATA-NHAc** further increases the E_{HOMO} to –4.81 eV. The susceptibility of the redox properties of the system to the peripheral substituent is exemplified by a large decrease (ΔE_{HOMO} = –0.28 eV) in the oxidation potential of **BATA-NHAc-NO_2** compared to all other members of the series. Ultimately, the oxidation properties observed for **TPA** are maintained for **BATA-NHAc**, however, some of the unwanted reaction pathways that occur when triarylamines are ionized, i.e., intramolecular carbazole formation at the aryl *o*-positions, are for structural reasons not possible which should be beneficial for increasing the stability of triaryl amines in the oxidized state.[23]

DFT calculations computed at the B3LYP-GD3BJ/6-31g(d) level were employed to gain further insight into the effect on the π-electronics of the uniquely twisted structure. The lowest-energy optimized structure of **BATA-NHAc** closely matches (bond length <3% discrepancy) the absolute structure determined by X-ray diffraction The amide groups significantly affect the energies (Figure 3) of the frontier molecular orbitals with a decrease in the band gap from **TPA** (E_g = 4.62 eV) to **TATA-NHAc** (E_g = 4.12 eV). Whereas **TATA-NHAc** has the HOMO distributed across all three aryl units, **BATA-NHAc** has the HOMO (E_{HOMO} = –4.57 eV) distributed on the two coplanar aryl rings, across the A- and B-plane. This extended π-conjugation explains the bathochromic shifts observed in the UV-vis spectra as well as the increased E_{HOMO} observed from the cyclic voltammogram of **BATA-NHAc** in comparison to all other controls. The LUMO (E_{HOMO} =–0.46 eV) of **BATA-NHAc** is positioned on the aryl unit in the C-plane and

is isolated with respect to the HOMO. These data confirm the twisting towards a C_2-axis facilitates a greater degree of planarization, and therefore increased π-conjugation, between the aryl units in the A- and B-plane, whilst simultaneously isolating the π-system in the C-plane. Furthermore, we calculated (uB3LYP-GD3BJ/6-31g(d)) the triplet energies of the frontier molecular orbitals (Figure 3). Both **BATA-NHAc** and **BATA-NHAc-NO$_2$** have low-lying triplet states at –3.01 and –3.45 eV, respectively, which makes them intriguing candidates for singlet-fission as $E^{S1} \geq 2E^{T1}$.[24] There is also potential for non-linear optical properties through functionalization of the segregated π-systems, i.e., from creating electron-rich and donor segments in a push-pull system.[25] Resultingly, these azatriseptanes systems may have applications in supramolecular chemistry[26] and functional materials,[27] and we are currently exploring these avenues within our laboratory.

In summary, we have developed a highly efficient method for the synthesis of a bench-stable ethane-bridged triphenylamine **BATA-NHAc** through a two-fold intramolecular Friedel-Crafts acylation, providing access to the first heterocycle containing three fused heptagon rings with a nitrogen at its core. This serves as an encouraging platform that provides an opportunity to attain highly strained polyseptanes. X-ray crystallography and DFT calculations revealed a contorted, helical, C_2-symmetric conformation with the strain mostly localized on the ethane bridges. **BATA-NHAc** demonstrated a red-shifted absorption compared to the strain-free derivative as well as concentration dependent emission profiles, which makes it an ideal candidate to explore the supramolecular behavior of these contorted hydrogen-bonding systems. In addition, synthetic access to polyseptanes should be an ideal platform from which to design access to larger, precisely doped negatively-curved nanographenes.

Acknowledgments The financial support from the University of Zurich for the purchase of the X-ray diffractometer used in this work is gratefully acknowledged. We also thank S. Jurt, T. Fox, and N. Bross for assistance with NMR measurements, the Mass Spectrometry Laboratory at the University of Zurich for MS measurements, and K. Gademann for generously hosting and supporting our research group. M.R. gratefully acknowledges funding from the Swiss National Science Foundation grant PZ00P2_180101. K.Z. thanks the China Scholarship Council for his Ph.D. fellowship. M.E.N thanks the Swiss Government Excellence Scholarship for her Ph.D. fellowship.

Author Contributions K.Z., P.A.H., M.E.N., and M.R. conceived, analyzed, validated, and visualized the work herein presented. K.Z., P.A.H, M.E.N., and M.R. carried out the investigation and developed the methodology. Funding was acquired by K.Z., M.E.N., and M.R., and resources by M.R. M.R. supervised the work. K.Z., P.A.H., M.E.N., and M.R. wrote the manuscript.

Keywords contorted π-systems, strain framework, polyseptanes, helical chirality, circulene analogs.

[1] a) S. H. Pun, Q. Miao, *Acc. Chem. Res.* **2018**, *51*, 1630–1642; b) I. R. Márquez, S. Castro-Fernández, A. Millán, A. G. Campaña, *Chem. Commun.* **2018**, *54*, 6705–6718; c) I. A. Stepek, K. E. Yamada, H. Ito, K. Itami, *Angew. Chem. Int. Ed.* **2021**, *60*, 23508–23532; *Angew. Chem.* **2021**,*133*, 23700–23724

[2] M. A. Majewski, M. Stępień, *Angew. Chem. Int. Ed.* **2019**, *58*, 86–116; *Angew.Chem*. **2019**,*131*, 90–122

[3] a) W. E. Barth, R. G. Lawton, *J. Am. Chem. Soc.* **1966**, *88*, 380–381; b) R. Bhola, T. Bally, A. Valente, M. K. Cyrański, Ł. Dobrzycki, S. M. Spain, P. Rempała, M. R. Chin, B. T. King, *Angew. Chem. Int. Ed.* **2010**, *49*, 399–402; *Angew.Chem.* **2010**,*122*, 409–412.

[4] K. Itami, G. G. Miera, S. Matsubara, H. Kono, K. Murakami, *Chem.Sci.* **2022**, *13*, 1848–1868

[5] a) L. T. Scott, E. A. Jackson, Q. Zhang, B. D. Steinberg, M. Bancu, B. Li, *J. Am. Chem. Soc.* **2012**, *134*, 107–110; b) J. Tomada, T. Dienel, F. Hampel, R. Fasel, K. Amsharov, *Nat. Commun.* **2019**, *10*, 1–10.

[6] A. Mackay, H. Terrones, *Nature* **1991**, *352*, 762–762.

[7] H. Terrones, in *Springer Handbook of Nanomaterials*, Springer, **2013**, pp. 83–104

[8] M. V. Diudea, C. L. Nagy, I. Silaghi-Dumitrescu, A. Graovac, D. Janežič, D. Vikić-Topić, *J. Chem. Inf. Model.* **2005**, *45*, 293–299.

[9] a) K. Hafner, G. L. Knaup, H. J. Lindner, *Angew. Chem. Int. Ed. Engl.* **1986**, *25*, 633–635; *Angew. Chem.* **1986**, *98 650–652*; b) K. Okada, H. Inokawa, T. Sugawa, M. Oda, *J. Chem. Soc., Chem. Comm.* **1992**, 448–449; c) K. Yamamoto, P. Pandit, S. Higashibayashi, *Chem. Eur. J.* **2017**, *23*, 14011–14016.

[10] a) K. Yamamoto, T. Harada, M. Nakazaki, T. Naka, Y. Kai, S. Harada, N. Kasai, *J. Am. Chem. Soc.* **1983**, *105*, 7171–7172; b) K. Yamamoto, T. Harada, Y. Okamoto, H. Chikamatsu, M. Nakazaki, Y. Kai, T. Nakao, M. Tanaka, S. Harada, N. Kasai, *J. Am. Chem. Soc.* **1988**, *110*, 3578–3584.

[11] K. Yamamoto, Y. Saitho, D. Iwaki, T. Ooka, *Angew. Chem. Int. Ed. Engl*. **1991**, *30*, 1173–1174; *Angew. Chem.* **1991**, *103*, 1202–1203.

[12] M. Hatanaka, *J. Phys. Chem. A.* **2016**, *120*, 1074–1083.

[13] M. Rickhaus, M. Mayor, M. Juríček, *Chem. Soc. Rev.* **2017**, *46*, 1643–1660.

[14] D. Kuck, A. Schuster, B.Ohlhorst, V. Sinnwell, A. de Meijere, *Angew. Chem. Int. Ed. Engl*. **1989**, *28*, 595–597; *Angew. Chem.***1989**,*101*, 626–628.

[15] a) G. Markopoulos, L. Henneicke, J. Shen, Y. Okamoto, P. G. Jones, H. Hopf, *Angew. Chem. Int. Ed.* **2012**, *51, 12884–12887; Angew. Chem.* **2012**, *124,13057–13060.*; b) M. Jevric, T. Zheng, N. K. Meher, J. C. Fettinger, M. Mascal, *Angew. Chem. Int. Ed.* **2011**, *50*, 717–719; *Angew. Chem.* **2011**,*123*, 743–745; c) P. Wagner, F. Rominger, T. Oeser, M. Mastalerz, *J. Org. Chem.* **2020**, *85*, 3981–3989.

[16] D. H. Huh, J. S. Jeong, H. B. Lee, H. Ryu, Y. G. Kim, *Tetrahedron* **2002**, *58*, 9925–9932.

[17] K. Ramachandran, A. Raja, N. Lingamurthy, M. S. Pandian, P. Ramasamy, S. V. Rao, *Chem. Phys. Lett.* **2020**, *742*, 137128.

[18] J. J. Armao IV, P. Rabu, E. Moulin, N. Giuseppone, *Nano Lett.* **2016**, *16*, 2800–2805.

[19] C. E. Colwell, T. W. Price, T. Stauch, R. Jasti, *Chem. Sci.* **2020**, *11*, 3923–3930.

[20] J. Rotzler, H. Gsellinger, A. Bihlmeier, M. Gantenbein, D. Vonlanthen, D. Häussinger, W. Klopper, M. Mayor, *Org. Biomol. Chem.* **2013**, *11*, 110–118.

[21] Y. M. Poronik, G. V. Baryshnikov, I. Deperasińska, E. M. Espinoza, J. A. Clark, H. Ågren, D. T. Gryko, V. I. Vullev, *Commun. Chem.* **2020**, *3*, 1–18.

[22] T. K. Ellis, M. Galerne, J. J. Armao IV, A. Osypenko, D. Martel, M. Maaloum, G. Fuks, O. Gavat, E. Moulin, N. Giuseppone, *Angew. Chem. Int. Ed*. **2018**, *57*, 15749–15753; *Angew. Chem.* **2018**, *130*, 15975–15979.

[23] P. Blanchard, C. Malacrida, C. Cabanetos, J. Roncali, S. Ludwigs, *Polym. Int.* **2019**, *68*, 589–606.

[24] M. B. Smith, J. Michl, *Chem. Rev.* **2010**, *110*, 6891–6936.

[25] N. Islam, A. H. Pandith, *J. Mol. Model.* **2014**, *20*, 1–17.

[26] J. F. Woods, L. Gallego, P. Pfister, M. Maaloum, A. Vargas Jentzsch, M. Rickhaus, *Nat. Commun.* **2022**, *13*, 1–8.

[27] a) A. Cesaretti, P. Foggi, C. G. Fortuna, F. Elisei, A. Spalletti, B. Carlotti, *J. Phys. Chem. C* **2020**, *124*, 15739–15748; b) M. Klikar, P. Solanke, J. Tydlitát, F. Bureš, *Chem. Rec.* **2016**, *16*, 1886–1905.